Nitric Oxide 93 (2019) 25–33

Contents lists available at ScienceDirect

Nitric Oxide

journal homepage: www.elsevier.com/locate/yniox

Nitric oxide-loaded chitosan nanoparticles as an innovative antileishmanial platform

Fernanda V. Cabral[a], Milena T. Pelegrino[b,c], Ismael P. Sauter[d], Amedea B. Seabra[b,c], Mauro Cortez[d], Martha S. Ribeiro[a,*]

[a] Center for Lasers and Applications, Nuclear and Energy Research Institute (IPEN-CNEN/SP), Av. Prof. Lineu Prestes, 2242, CEP 05508-000, São Paulo, SP, Brazil
[b] Center for Natural and Human Sciences, Universidade Federal do ABC, Av. dos Estados 5001, CEP 09210-580, Santo André, SP, Brazil
[c] Nanomedicine Research Unit (NANOMED), Universidade Federal do ABC, Santo André, SP, Universidade Federal do ABC, Av. dos Estados 5001, CEP 09210-580, Santo André, SP, Brazil
[d] Institute of Biosciences, University of São Paulo (ICB/USP), Avenida Prof. Lineu Prestes, 1374, CEP 05508-000, São Paulo, SP, Brazil

ARTICLE INFO

Keywords:
Bioluminescence
Cutaneous leishmaniasis
Immunofluorescence
Leishmania (L.) amazonensis
Macrophages
S-nitrosothiols

ABSTRACT

Leishmaniasis is a neglected tropical disease that demands for new therapeutic strategies due to adverse side effects and resistance development promoted by current drugs. Nitric oxide (NO)-donors show potential to kill *Leishmania* spp. but their use is limited because of their instability. In this work, we synthesize, characterize, and encapsulate S-nitroso-mercaptosuccinic acid into chitosan nanoparticles (NONPs) and investigate their activity on promastigotes and intracellular amastigotes of *Leishmania (Leishmania) amazonensis*. Cytotoxicity on macrophages was also evaluated. We verified that NONPs reduced both forms of the parasite in a single treatment. We also noticed reduction of parasitophorous vacuoles as an evidence of inhibition of parasite growth and resolution of infection. No substantial cytotoxicity was detected on macrophages. NONPs were able to provide a sustained parasite killing for both *L. (L.) amazonensis* infective stages with no toxicity on macrophages, representing a promising nanoplatform for cutaneous leishmaniasis.

1. Introduction

Leishmaniasis consists in a group of neglected tropical diseases that are endemic in 97 countries around the world and affects approximately 12 million people worldwide [1,2]. They are caused by protozoan parasites of the genus *Leishmania* and transmitted by the bite of female hematophagous sandflies during the blood meal [1]. According to the World Health Organization, nearly 0.6 to 1 million new cases of the cutaneous form appear worldwide annually, mostly in the Americas, Mediterranean, Middle East and Central Asia [1,3].

The tegumentary forms promote extensive ulcerated and destructive lesions on the exposed parts of the body. Since it is a chronic illness, long periods of treatment are required and most of the times the unsightly lesions can lead to a permanent scar producing a psychological impact on patients [4,5].

The current available treatments are limited, once the antileishmanial drugs are expensive and toxic, which may produce many adverse side effects [6]. Also, the parasite drug resistance has become widespread that contributes to a lack of effective treatments [6,7]. Therefore, considering a major public health problem, a strategic framework for leishmaniasis control is urgently needed with alternatives and new cost-effective therapies that provide better outcomes and quality of life for patients.

Nitric oxide (NO) plays a key role in different biological systems, including leishmanial infections. The outcome of leishmaniasis has been related to increase of specific T helper cells leading to Th1 (resistance) or Th2 (susceptibility) response [8]. Th1 cells prompts the expression of inducible nitric oxide synthase (iNOS) by macrophages. This enzyme catalyzes the oxidation of the guanidine nitrogen of L-arginine to generate NO, which kills the parasite. On the other hand, the Th2 response inhibits NO production besides activates macrophages to produce arginase, which competes with iNOS for the same substrate

Abbreviations: BMDM, bone marrow-derived macrophages; CS, chitosan; NPs, nanoparticles; MSA, mercaptosuccinic acid; NONPs, NO-releasing nanoparticles; TPP, sodium tripolyphosphate; PDI, polydispersity index; S-nitroso-MSA, S-nitroso-mercapsotosuccinic acid; AFM, atomic force microscopy; PBS, phosphate buffer saline; FBS, fetal bovine serum; MTT, (3-[4,5-dimethyl-2-thiazolyl]-2,5-diphenyl-2Htetrazolium bromide; BSA, bovine seric albumin; TBS, tris-buffer saline; PV, parasitophorous vacuole; UV–Vis, ultraviolet–visible

* Corresponding author.
E-mail address: marthasr@usp.br (M.S. Ribeiro).

https://doi.org/10.1016/j.niox.2019.09.007
Received 4 April 2019; Received in revised form 4 September 2019; Accepted 17 September 2019
Available online 18 September 2019
1089-8603/ © 2019 Elsevier Inc. All rights reserved.

[8]. In fact, several studies have demonstrated the NO role to control Leishmania spp. *in vitro* and *in vivo* [9–12].

The NO high reactivity and short half-life requires the use of NO donors as sources of NO [13]. NO donors such as S-nitroso-N-acetyl-*L*-cysteine, S-nitrosoglutathione, S-nitrosothiols and sodium nitroprusside have been explored as an alternative treatment for tegumentary leishmaniasis [14–16]. However, NO donors are commonly unstable and easily decomposed when exposed to light and high temperatures. They provide a fast NO-releasing and may reduce its effectiveness and increase cytotoxicity [13,14,17].

The recent advances in nanotechnology have brought several advantages of nanoparticles as a nanocarrier-based drug delivery system to overcome conventional treatments of cutaneous leishmaniasis [18]. The drug-loaded nanoparticles are able to promote a gradual and sustained drug release improving biodistribution, stability, solubility and decreasing undesirable cytotoxicity [19].

Chitosan (CS) is known as a hydrophilic polysaccharide with antimicrobial activity [20]. Particularly, chitosan nanoparticles (NPs) have been successfully used to carry and delivery drugs in different branches of health sciences [21,22]. Thus, we synthesized, characterized and encapsulated NO donor S-nitroso-mercaptosuccinic acid (S-nitroso-MSA) into CS NPs (Fig. 1) and investigated their activity on promastigotes and intracellular amastigotes of *Leishmania (Leishmania) amazonensis*, which cause cutaneous and mucocutaneous leishmaniasis. Herein, we showed that NO-releasing nanoparticles (NONPs) were able to decrease both forms of parasites without affecting macrophage viability. More importantly, we observed the decrease of parasitophorous vacuoles (PV), which denotes the resolution of infection.

2. Material and methods

2.1. NPs synthesis

MSA, the precursor of NO donor molecule, was encapsulated into NPs by the addition of MSA in CS solution during NP synthesis, as previously described [17,23,24]. Briefly, an aqueous solution of CS (1.0 mg/mL) and MSA (66.67 mM) was dissolved in 1% acetic acid at room temperature. After 90 min of magnetic stirring, a sodium tripolyphosphate (TPP) solution at 0.6 mg/mL was dropwise added to previous prepared CS/MSA solution. The final mixture was magnetically stirred for at least 120 min to form NPs containing MSA, henceforward named NPs.

2.2. Characterization of NPs

The average hydrodynamic diameter (% by intensity), polydispersity index (PDI) and zeta potential of NPs were evaluated by dynamic light scattering using a Nano ZS Zetasizer (Malvern Instruments Co, UK) [25]. The encapsulation efficiency of MSA into NPs was determined by the titration of the free thiol group of MSA with 5,5-dithio-bis-(2-nitrobenzoic acid), as previously described [23,24].

To investigate their shape and morphology, topography and phase contrast images of NPs were simultaneously obtained by atomic force microscope (AFM, AFM/SPM Series 5500, Agilent, USA) in tapping mode.

2.3. Nitrosation of free or encapsulated MSA

Thiol group of free or encapsulated MSA (50 mmol L^{-1}) was nitrosated by adding an equimolar amount of sodium nitrite ($NaNO_2$) leading to the formation of free or encapsulated S-nitroso-MSA, henceforward named S-nitroso-MSA and NONP, respectively. Fig. 1 shows the schematic representation of the formation of MSA-containing CS NPs, followed by the nitrosation of MSA, yielding S-nitroso-MSA containing CS NPs (NONPs). The formation of free or encapsulated S-nitroso-MSA was confirmed by the appearance of the characteristic S–NO group absorption bands at either 336 nm (ε = 980.0 L mol^{-1} cm^{-1}) or at 545 nm (ε = 18.4 L mol^{-1} cm^{-1}) using the UV–Vis spectrophotometer (Agilent 8454, Palo Alto, CA, USA).

2.4. In vitro kinetics of NO release

The NO release profile from free and encapsulated S-nitroso-MSA was measured in deionized water monitored by UV–Vis spectrometry [17,23]. The initial concentration of S-nitroso-MSA (free or encapsulated) was 50 mM. Kinetic data were obtained by measuring changes in absorbance intensity of S-nitroso-MSA at 545 nm (nN → π* transition), by using the UV–Vis spectrophotometer (Agilent 8454, Palo Alto, CA, USA), with a temperature controlled sample holder. Changes at 545 nm are solely associated with S–N bond cleavage and free NO release [17,23]. Kinetic data were collected in 60 min intervals at 37 °C for 10 h. The quantity of NO released over time was calculated according to Beer's law [23].The initial rates of NO release from S-nitroso-MSA and from NONPs were determined through linear regression of the initial sections (0–3 h range) of the kinetic curves [26].

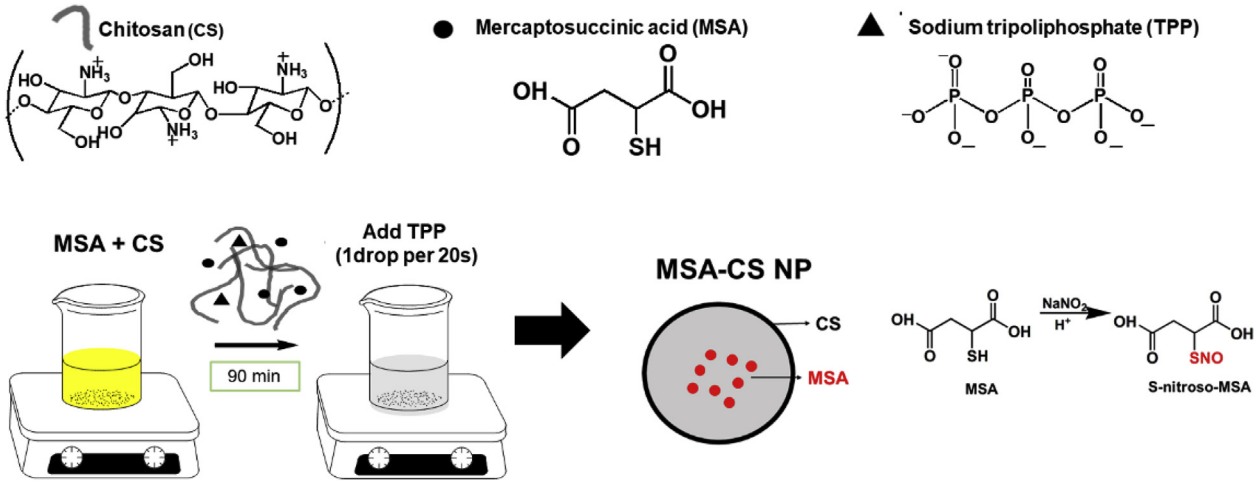

Fig. 1. Schematic representation of the preparation of MSA containing CS NPs, followed by the nitrosation of thiol group of MSA, leading to the formation of S-nitroso-MSA containing CS NPs, henceforward named (NONPs).

2.5. Parasite culture

Leishmania (L.) amazonensis (MHON/BR/73/2269, transgenic line expressing luciferase) was a kind gift from Prof. Silvia R. B. Uliana (University of São Paulo). Promastigotes were grown at 25 °C in M199 medium (Sigma-Aldrich, USA) supplemented with 10% fetal bovine serum (FBS, GibcoTM Invitrogen Corporation, USA) and 0.25% hemin (Sigma-Aldrich, USA) with pH 7.2 [27]. To obtain lesion amastigotes, female BALB/c mice were infected in footpad with 1×10^6 promastigotes. After 8 weeks, the animals were euthanized and the parasites recovered from footpad lesions. The lesion homogenate was submitted to sequential 200 g centrifugation steps to separate parasites from tissue debris [28].

2.6. Activity of NONPs on Leishmania promastigotes

Leishmania promastigotes (5×10^6 per well) were treated with increasing concentrations (25–200 μM) of NONPs and NPs for 24 h. In this manuscript, the molar concentrations refer to the molar concentrations of MSA for NPs, and S-nitroso-MSA for NONPs. Metabolic activity was determined through luciferase assay using luciferin as a substrate to promote bioluminescence reaction (One Glo Luciferase Assay System, Promega Corporation, USA). This system provides a sensitive, robust and homogeneous assay for detection of firefly luciferase reporter gene expression in recombinant cells by bioluminescence. Bioluminescence is a phenomenon that involves light emission mediated by ATP in living organisms. Luciferin was added to wells 5 min before bioluminescence detection by a spectrophotometer (Spectramax M4, Molecular Devices, USA). Then, the 50% and 90% inhibitory concentrations (IC_{50}, IC_{90}) were calculated. Parasite kinetics following treatments was determined as described above and results were acquired at 3, 6, 12 and 24 h after incubation.

Additionally, parasites (1×10^5) were treated with increasing drug concentrations (25–400 μM) of NONPs and NPs for 24 h. Afterwards, parasite metabolic activity was determined daily during 5 days.

2.7. Cytotoxicity assays on macrophages

All the experiments were carried out in accordance with internationally recognized guidelines and in agreement with the Brazilian Federal Law 11,794, Decree 6899 and on the Normative Resolutions published by the National Council for the Control of Animal Experimentation (CONCEA), and approved by the Ethic Committee on Animal Use of the IPEN-CNEN/SP under the protocol number 189/17.

Bone marrow-derived macrophages (BMDM) from BALB/c mice were obtained and cultured for 7 days in RPMI 1640 medium (15 mM HEPES, 2 g of sodium bicarbonate/L, and 1 mM L-glutamine) and supplemented with 20% FBS and 20% *L*-929 cell conditioned medium (LCCM) [28,29].

For mitochondrial activity assay, cells (8×10^4) were plated on 96-well plates 24 h prior experiments and then treated with increasing concentrations (0–400 μM) of NONPs and NPs for 24 and 48 h and their viability was evaluated by MTT. Briefly, after treatment, the cells were incubated with 30 μL of MTT (at 5.0 mg/mL) (3-[4,5-dimethyl-2-thiazolyl]-2,5-diphenyl-2H-tetrazolium bromide; Sigma-Aldrich, USA) and maintained at 37 °C for 4 h. The reaction was stopped by adding 30 μL of 20% (w/v) sodium dodecyl sulfate (SDS) to each well and the optical density was measured in a spectrophotometer (Spectramax M4, Molecular Devices, USA) at 595 nm using a reference wavelength of 690 nm. Results were expressed as a percentage of mitochondrial activity compared to control [30].

For immunofluorescence, 2×10^5 cells per well were plated on glass coverslips in 24-well plates and treated with 400 μM NONPs and NPs 24 h after. Forty eight-h post-treatment, the cells were fixed with methanol, washed with PBS, and permeabilized/blocked with 0.1% Saponin (Sigma-Aldrich, USA) and BSA (bovine seric albumin, Sigma-Aldrich, USA) in TBS (tris-buffer saline). Coverslips were incubated for 1 h with 10 μg/ml DAPI. Images were obtained with a fluorescence microscope (DMI6000B/AF6000, Leica, Germany) connected to a digital camera system (DFC 365 FX, Leica, Germany) and processed by ImageJ software. The average number of adhered cells was quantified by counting at least 20 fields per coverslip [28,31].

2.8. Activity of NONPs on intracellular amastigotes

Macrophages (8×10^4) were plated on 96-well plates (bioluminescence) or 2×10^5 per well on glass coverslips in 24-well plates (immunofluorescence) 24 h prior experiments and then infected with lesion amastigotes (multiciplicity of infection = 5) for 1 h at 34 °C. Cells were washed and incubated in fresh medium for 24 h. Infected cells were treated with 400 μM of NONPs and NPs. The supernatant of infected and treated cells was removed to quantify the NO production. Parasite metabolic activity of infected cells was quantified by bioluminescence and the number of parasites was quantified by counting through fluorescence microscopy. For this, the cells were fixed with methanol, washed with PBS, and permeabilized/blocked with 0.1% Saponin and BSA in TBS. Coverslips were incubated for 2 h with rabbit polyclonal antibodies against *Leishmania*, followed by anti-rabbit IgG Alexa Fluor 488 (Molecular Probes, USA). Rat anti-mouse Lamp1 mAb (BD Biosciences, USA) was used to stain vacuolar-associated protein, being incubated for 2 h and then for 1 h with anti-rat IgG Alexa Fluor 568 (Molecular Probes, USA). Nuclei were stained with 10 μg/mlL DAPI for 1 h. Images were obtained with fluorescence microscopy and processed by ImageJ software [28,31]. Results were determined by counting 300 cells per coverslip and expressed as percentage of infected macrophages and average number of amastigotes per macrophage. The infection index was also calculated following the formula:

$$\frac{\text{Number of amastigotes}}{\text{infected macrophages}} \text{ x \% infection}$$

2.9. Nitric oxide detection

To determine NO production, nitrite in the infected cell supernatant was detected by the Griess reagent (1% sulfanilamide, 0.1% *N*-naphthyl-ethylenediamine, 2.5% ortho-phosphoric acid) at room temperature for 15 min. The NO concentration was determined by preparing a sodium nitrite standard curve. Absorbance was measured in a spectrophotometer at 540 nm [32].

2.10. Statistical analysis

All data are representative of at least three independent assays in triplicate, unless stated otherwise. Statistical analysis was performed using GraphPad Prism 6.0 software by one-way ANOVA followed by the Tukey post-test. Differences were considered statistically significant when $p < 0.05$.

3. Results

3.1. Characterization of NPs

A spherical morphology of NPs was evaluated by AFM images, Fig. 2A exhibits a representative image of NP with a homogenous distribution. Fig. 2B exhibits a size lognormal distribution with an average size of 42.10 ± 1.37 nm at solid state.

The hydrodynamic size, PDI, and zeta potential of NPs were 130.3 ± 1.3 nm, 0.28 ± 0.01 and +29.4 ± 1.07 mV, respectively. The encapsulation efficiency of MSA into the nanoparticles was 98.9%. NPs are stable in deionized water for approximately 6 months.

Thiol group of free or encapsulated MSA was nitrosated by reacting

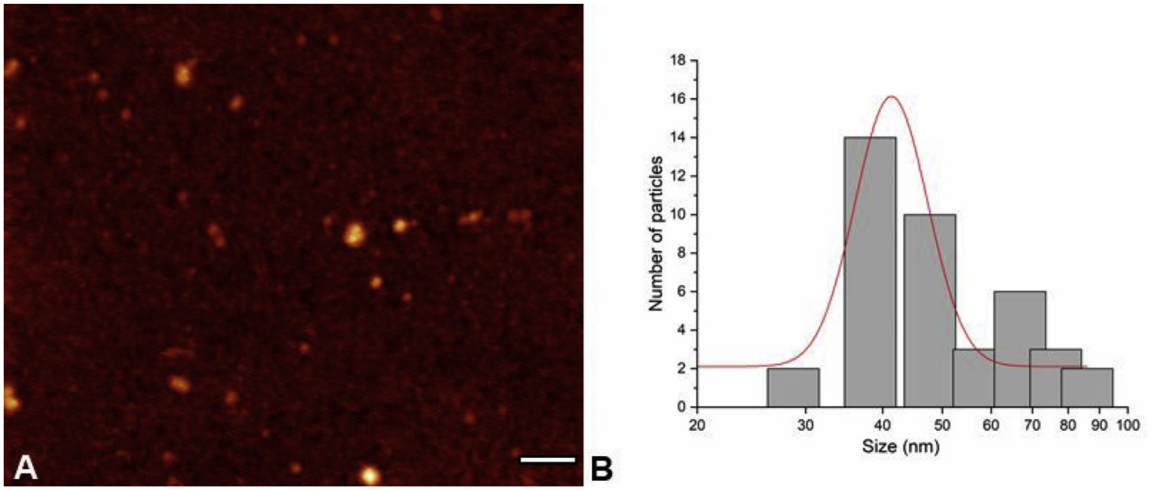

Fig. 2. Representative atomic force microscopy (AFM) topography image (A) and size lognormal distribution of NPs (B). Bar represents 200 nm.

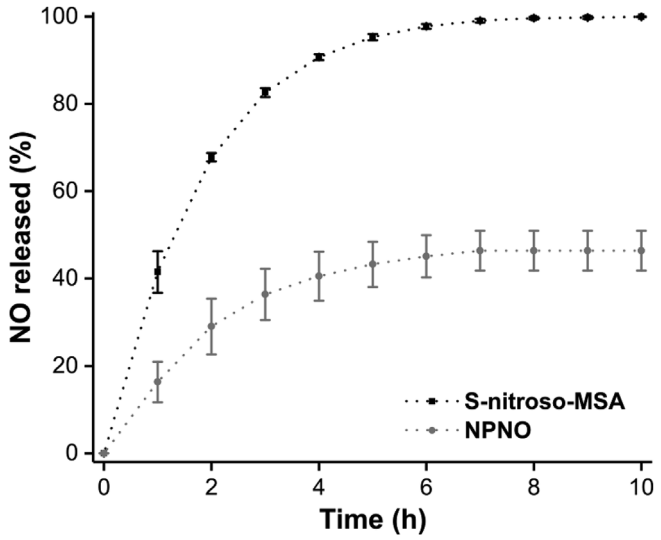

Fig. 3. Kinetics of NO release from free and encapsulated S-nitroso-MSA measured in deionized water and monitored by UV–Vis spectrometry (initial concentrations of NO donor were 50 mM in both curves) at 37 °C. The results are reported as the mean ± standard deviation (SD) of three independent experiments.

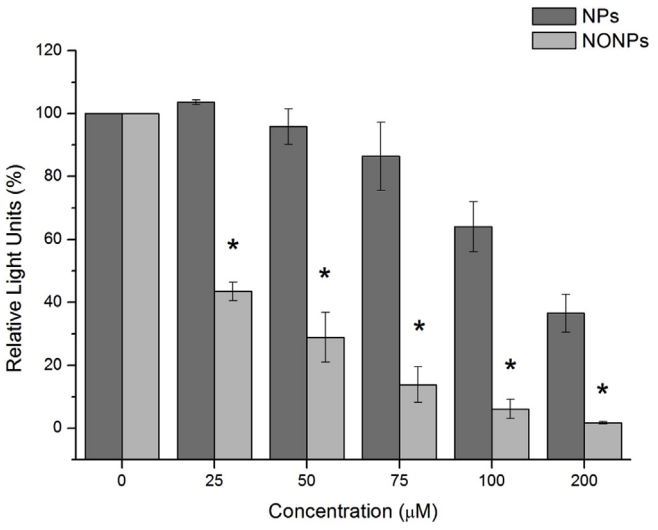

Fig. 4. Dose-response of NPs and NONPs from 0 to 200 μM against *L.(L.) amazonensis* promastigotes determined by bioluminescence assay 24 h after treatment. Data represent mean values ± standard error of the mean (SEM). Statistically significant differences were observed for concentrations higher than 25 μM compared to their counterparts (*, $p < 0.05$) ($n = 6$).

with equimolar amount of $NaNO_2$ leading to formation of free or encapsulated S-nitroso-MSA, respectively. The kinetics of NO release from free and encapsulated S-nitroso-MSA is shown in 3. We can observe the presence of two stages of NO release profile: an initial burst in the first 3 h of monitoring, following by the establishment of *a plateau* for at least 10 h, for both curves. The initial rates of NO release for free and encapsulated S-nitroso-MSA were 16.0 ± 2.8% h^{-1} and 10.2 ± 1.3% h^{-1}, respectively. For free S-nitroso-MSA *ca.* 100% of NO is released upon the establishment of the steady-state. In contrast, 45% of NO is released from NONPs. These results indicate the sustained release of NO upon the encapsulation of the NO donor into CS NPs. Nitrosation was performed immediately before all experiments.

3.2. NONPs decrease promastigotes of L. (L.) amazonensis

NPs affected *Leishmania* promastigotes, promoting 65% parasite killing at 200 μM. When NONPs were used, we observed a more pronounced dose-dependent parasite killing, with a reduction of approximately 50% of the promastigote population at 25 μM, reaching approximately 85% of promastigote reduction at 75 μM (Fig. 4).

The more evident decreasing signal for NONPs was noticed at 100 and 200 μM with 94% and 98% parasite killing, respectively (see Fig. 4). As a result, we were able to determine the IC_{50} at 31.5 and IC_{90} at 102.4 μM, according to the exponential fitting of the dose-response curve (Fig. 5).

Following NP treatment, we noted that proliferation of the remaining parasites was slightly affected (Fig. 6A). Nevertheless, a drastic influence on parasite recovery after NONP was observed. In fact, the higher the concentration, the higher the parasite reduction (Fig. 6B).

To demonstrate the total clearance of parasites, we plotted the parasite growth with more days of culture (Fig. 7). Although there was nearly 98% promastigotes inhibition after NONPs treatment at 200 μM (Fig. 6B), we observed a parasite recovery 3 days post-treatment, which was not visualized in 400 μM treated-parasites (Fig. 7). Actually, we observed a statistically significant difference with this last concentration 3 days post-treatment when compared to control. Thus, we included the 400 μM concentration for further studies.

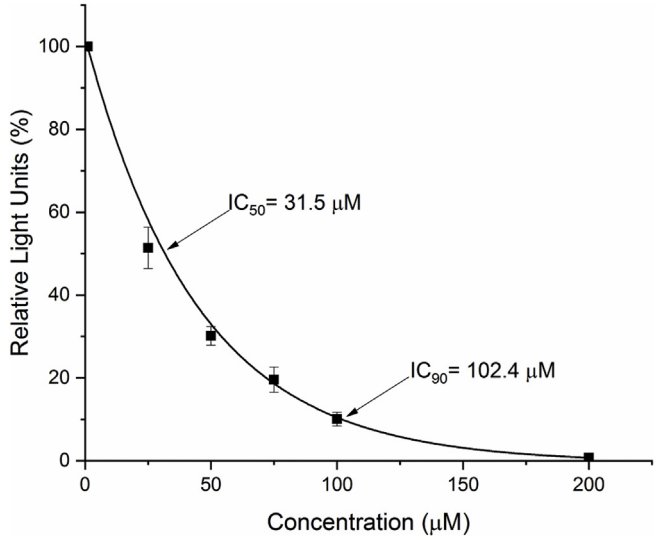

Fig. 5. Dose-response fitting curve of NONPs on *Leishmania (L.) amazonensis* promastigotes. Parasites were treated with increasing concentrations of NONPs (0–200 μM) for 24 h. Values shown represent the mean ± SEM (n = 6).

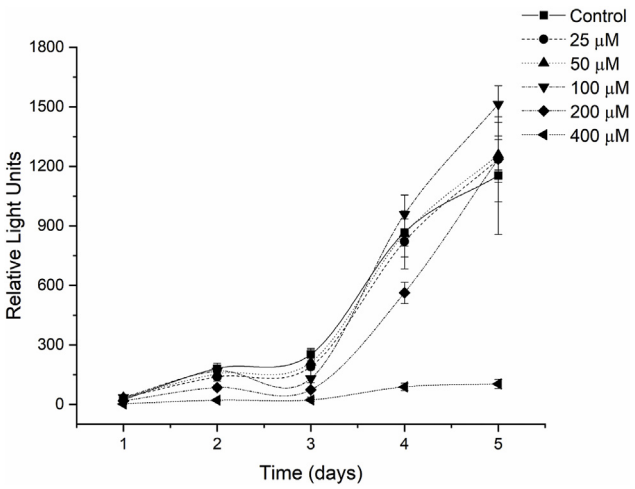

Fig. 7. *Leishmania (L.) amazonensis* promastigotes proliferation until 5 days post-treatment with different concentration (0–400 μM) of NONPs determined by bioluminescence assay. Statistically significant difference was observed for 400 μM compared to control after day 3 ($p < 0.05$). Values show means ± SD (n = 3).

3.3. Treatment with NONPs is not toxic to macrophages

When mitochondrial activity of NONPs was measured by MTT in macrophages, no effect was observed in all concentrations tested at different times of incubation (Fig. 8). Twenty four-h after incubation, we noticed about 80% of macrophages were viable at concentrations up to 200 μM. In addition, the highest concentration of 400 μM maintained cell viability around 75% even after 48 h (Fig. 8).

In fact, typical phenotype macrophage morphology remains similar when treated with NONPs or NPs compared to the untreated cells (Fig. 9). More important, the number of macrophages per field is identical in all treatments (control: 24.6 ± 3.7, NPs: 23.7 ± 5.4 and NONPs: 24.1 ± 2.3), confirming the results shown in Fig. 8.

3.4. Intracellular amastigotes of L. (L.) amazonensis are susceptible to NONPs

Regarding the release of the NO-donor from NPs, undetectable levels of nitrite were obtained in untreated or NP-treated (400 μM) infected macrophages. However, high levels of nitrite reaching approximately 300 μM were detected in the supernatant when the infected cells were treated with NONPs (Fig. 10), demonstrating stability and a high level of the toxic NO compound along the infection.

Next, we quantified the anti-leishmanial effect of NONPs in intracellular amastigotes of *L. (L.) amazonensis* by two experimental methods. We observed a decrease of about 33% in intracellular amastigotes when compared to the untreated control and NP samples by bioluminescence after 24 h of NONPs incubation (Fig. 11).

Furthermore, 48-h after treatment, NPs were able to reduce the number of amastigotes per macrophages and the infection index in about 21% and 33%, respectively, when intracellular parasite susceptibility was analyzed by immunofluorescence. In contrast, NONPs promoted a more evident and sustained effect, reducing in about 47% and 56% the number of intracellular amastigotes and its infection index, respectively. There was no significant difference in the percentage of infection when compared to the control, although approximately a 10% reduction was observed in both treated groups (Table 1).

The enhanced leishmanicidal effect of NONPs on intracellular amastigotes is easily visualized inside macrophages as shown in Fig. 12. Untreated control infected macrophages showed numerous amastigote

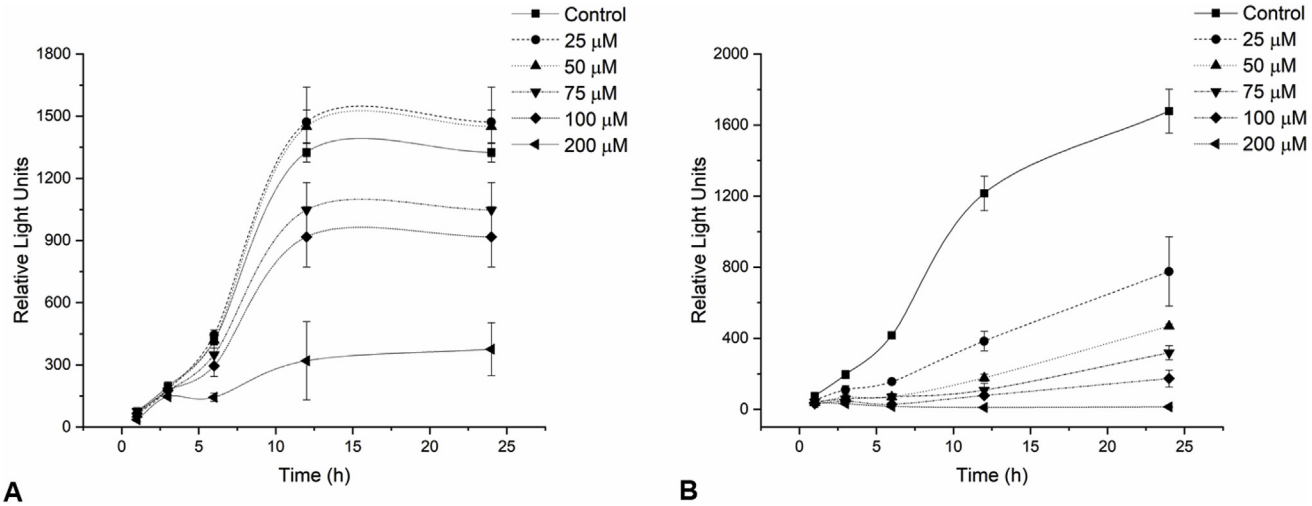

Fig. 6. *Leishmania (L.) amazonensis* promastigotes metabolic activity from 0 to 24 h post-treatment with different concentrations (0–200 μM) of NPs (A) and NONPs (B) determined by bioluminescence assay. Values show means ± SD (n = 3).

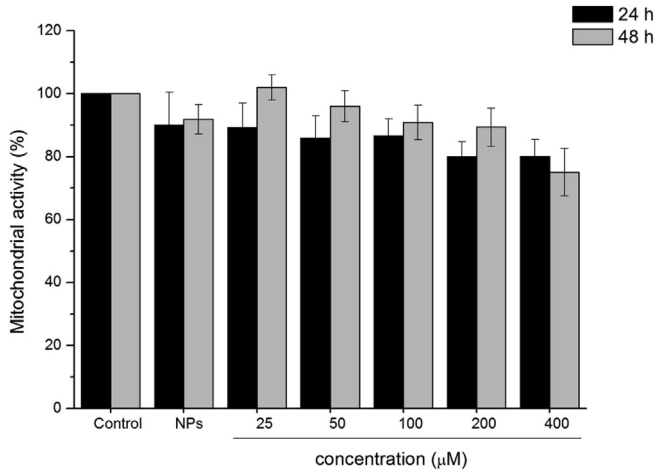

Fig. 8. BMDM treated with increasing concentrations of NONPs (0–400 μM) and NPs (400 μM) for 24 h and 48 h. Mean values ± SEM of mitochondrial activity were determined by MTT assay. No statistically significant differences were noticed (n = 9).

forms inside large lysosomal structures called parasitophorous vacuole (PV) with 48 h of infection. When infected macrophages were treated with NPs, we can perceive a smaller number of amastigotes inside PV compared to control. On the contrary, it is possible to recognize not only a reduction in the number of intracellular amastigotes but also in the size of the *Leishmania*-PV following NONPs treatment, which supports the killing effect of this compound on intracellular parasites.

4. Discussion

This study showed that NONPs are able to reduce promastigotes and intracellular amastigotes of *L. (L.) amazonensis* with no substantial macrophage cytotoxicity.

The hydrodynamic size and PDI of NPs described here are in accordance with other studies reported in literature [33,34]. The encapsulation efficiency of MSA into NPs was higher than reported in literature, which indicates a successful formation of NPs due to positive interactions between the nanoparticle components (CS and TPP) and MSA [34,35].

The positive zeta potential indicates that NPs are positively charged and it is related to amino groups presented in CS structure. In fact, Lima and co-workers have showed chitosan-based silver nanoparticles with positive zeta potential [19]. In addition, our results are similar to those reported by Pelegrino et al. [23].

The AFM image showed the formation of spherical nanoparticles with a lognormal size distribution, similar to size distribution reported by other authors [33,35]. It should be noted that nanoparticle size at solid state is usually smaller compared with hydrodynamic size distribution, as reported here, due to the presence of water solvation layers on the nanoparticle surface. In addition, our results demonstrated that NO can be released from the NPs. Similar results were previously reported by Pelegrino and collaborators [23].

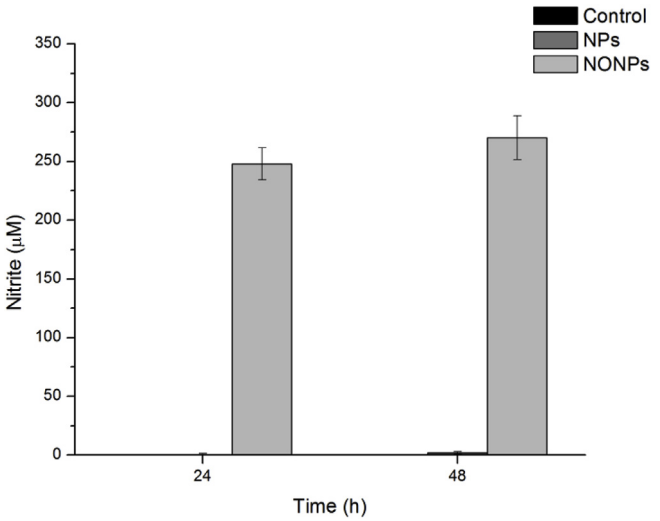

Fig. 10. Intracellular amastigotes were treated with NPs and NONPs (400 μM) and the amount of nitrite was determined by the supernatant of the infected macrophages using the Griess reagent. Values show means ± SD of nitrite detection (n = 6).

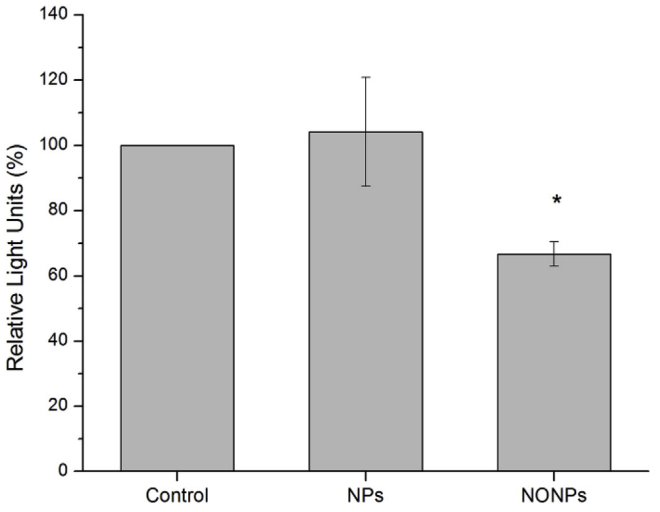

Fig. 11. Metabolic activity of intracellular amastigotes of *L. (L.) amazonensis* treated with NPs and NONPs at 400 μM for 24 h and determined by luciferase assay. Data represent mean values ± SD. Statistically significant differences were observed between NONPs and other groups (*, $p < 0.05$) (n = 3).

By monitoring the thermal stability of S-nitroso-MSA, and thus the NO release profile, the encapsulation of the NO donor significantly decreased the rates of NO release (see Fig. 3). As previously observed, a sustained NO release can be achieved upon the encapsulation of the NO donor, in this case S-nitrosothiol, into a nanocarrier. Similar results were reported for different classes of NO donors encapsulated into polymeric nanoparticles [36–38], microemulsions [39], and hydrogels

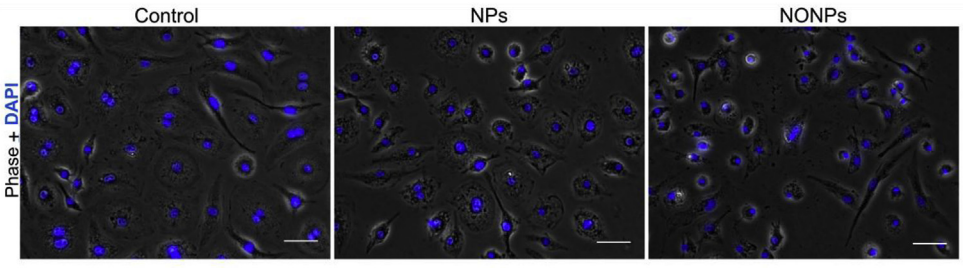

Fig. 9. Immunofluorescence staining representative images of BMDM treated with NPs and NONPs (400 μM) for 48 h. Nuclei were stained with DAPI (blue fluorescence). Images were processed by ImageJ software and the average number of adhered cells was quantified by counting at least 20 fields per coverslip. Bars represent 25 μm (n = 6).

Table 1
Activity of NPs and NONPs on intracellular amastigotes of *Leishmania (L.) amazonensis*. Results were determined by counting 300 cells per coverslip and expressed as percentage of infected macrophages and average number of amastigotes per macrophage. The infection index was also calculated following the formula: *Number of amastigote/macrophage x % of infected macrophage*. * denotes statistically significant differences between NPs and NONPs. ** denotes statistically significant differences between control and NONPs ($p < 0.05$, $n = 6$).

	Number of intracellular amastigotes/infected macrophage	% Infection	Infection Index
Control	8.5 ± 1.2	76.2 ± 7.1	649.7 ± 115.1**
NPs	6.7 ± 0.2*	65.1 ± 3.1	436.0 ± 6.9
NONPs	4.5 ± 0.4*	63.7 ± 5.4	288.0 ± 39.9**

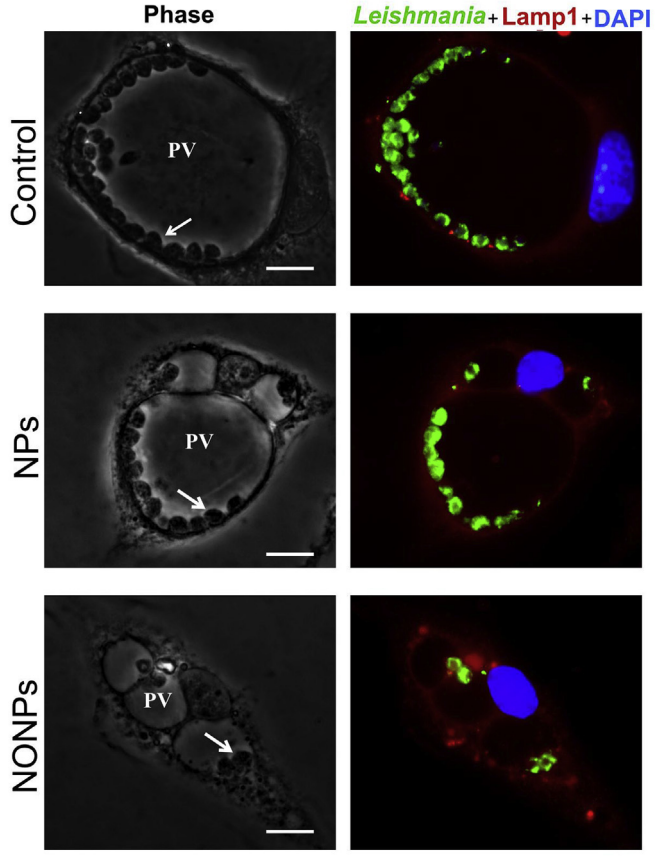

Fig. 12. Phase contrast and immunofluorescence staining representative images of infected macrophages treated with NPs and NONPs at 400 μM after 48 h. Nuclei were stained with DAPI (blue fluorescence) and parasites stained with rabbit polyclonal antibodies against amastigotes of *Leishmania (L.) amazonensis*, followed by anti-rabbit IgG (green fluorescence). Rat anti-mouse Lamp1 mAb was used to stain vacuolar-associated protein and then anti-rat IgG was used (red fluorescence). Images were processed by ImageJ software and results determined by counting 300 cells per coverslip and expressed as percentage of infected macrophages and average number of amastigotes per macrophage. Bars represent 10 μm. Arrows indicate amastigote inside macrophage (n = 6).

[40].

Chitosan is an attractive platform to encapsulate NO donors due to inherent characteristics as biocompatibility, biodegradability, non-toxicity to mammal cells, high bioavailability, and ease of transformation [41]. It is a positively charged polymer with free amino groups capable of interacting with anionic molecules [20,21]. To the better of our knowledge, this is the first study to show that S-nitrosothiol-loaded CS NPs promote antileishmanial activity.

As the parasite membrane contains negatively charged phospholipids [42], an antileishmanial activity was already expected with NPs due to antimicrobial activity of chitosan [20]. However, the antiparasitic effect was significantly enhanced in the presence of NO donor, demonstrating a treatment improvement achieved by its association.

In addition, we observed a dose-dependent promastigote decrease following NONP treatment. In fact, IC_{50} value was achieved 31.5 μM. Although this value is higher than IC_{50} for amphotericin B or miltefosine, NONPs showed no toxicity on macrophages up to 400 μM. Besides, NONPs were formulated to be applied as a topical treatment unlike current antileishmanial drugs. Thus, no systemically toxicity is expected.

At the highest concentration (200 μM) we noticed a significant parasite recovery 3 days after treatment (see Fig. 7). Although this dose was almost 2 times greater than IC_{90}, we should consider that IC_{90} represents a single point on the dose-response curve in the first 24 h, and the remaining parasites were still able to keep proliferating. Thus, we hypothesize that the use of a higher dose (400 μM) could support parasite reduction for longer periods. This hypothesis was confirmed and we observed a noticeable and sustained promastigote killing even after 5 days, which corroborates with other studies, where high levels of NO were necessary to promote an efficient antiparasitic activity [43–45].

Before evaluation of drug efficiency against intracellular amastigotes, we evaluated the toxicity of NONPs on macrophages. In fact, when promastigotes are inoculated in the host by the bite of the sandfly, they are phagocytized by macrophages, where they will be able to differentiate into amastigote forms [46]. Although a slight cell viability diminution has been noted following NONP administration at 400 μM our results demonstrated no significant toxicity on macrophages even at high concentrations.

NO donors, such as S-nitrosothiols, are usually considered cytotoxic at high concentrations due to the free and uncontrolled NO-releasing [15,44]. Our results provide substantial evidence that chitosan nanoparticles could be considered a promising drug delivery strategy. Probably the NO-loaded chitosan nanoparticles reduced the cytotoxic effects providing a sustained, controlled and gradual NO-releasing and, consequently, no noteworthy decrease of macrophages and cell morphological alterations were perceived even at 400 μM.

We then proceeded with experiments using free and NONPs at 400 μM. Firstly, we verified high levels and stability of nitrite along infection following NONP administration. After, we realized that about 33% of the intracellular amastigotes decreased with a single NONP treatment. Forty eight-h after, a further killing around 50% was observed. It is worth to highlight that NONP even at 400 μM did not show significant toxicity to macrophages following 24 or 48 h of the treatment.

Indeed, S-nitrosothiols are endogenous molecules known not only because of their ability to release NO, but also because of other biological functions such as transnitrosation and S-thiolation [47]. Transnitrosation reaction occurs by the transfer of nitrosothiols to a molecule or protein containing cysteine residues, which generates cytotoxicity by an enzymatic inhibition [15,48]. For this reason, *Leishmania* cysteine proteinase activity is probably inhibited by NO-donors through transnitrosation reaction leading to parasite death [16]. Besides, the NO interaction directly with both parasites stages may compromise their proliferation because of mitochondrial respiratory chain disorder generated by iron depletion and aconitase inhibition [16,49].

Promastigotes are more susceptible to NO than amastigote stages, particularly regarding *L. (L.) amazonensis*, probably explained by their ability to survive in the hostile environment inside macrophages [43,50]. The amastigote forms of *L. (L.) amazonensis* usually replicate inside large PVs that expand during infections and this is extremely related to the parasite virulence, disease severity and the competence to survive and proliferate inside the host cells [51,52].

We noticed several amastigotes within a large PV in the control group, which indicates significant infection progress [50] (see Fig. 11). Likewise, although there was a parasite burden reduction after NP administration, the PV size and morphology seem to be similar to control. On the contrary, NONP treatment showed a remarkable PV size reduction and intracellular parasite killing.

Small PVs are not able to sustain the parasite growth [50]. In contrast, large PVs are capable of diluting the antimicrobial agents such as reactive oxygen species and reactive nitrogen species improving the amastigote survival [50,51]. Thus, treatments that can reduce PVs reveal a great advantage against *L. (L.) amazonensis*. In fact, the PV size in this study brings crucial evidence that infection resolution can be happening because of the sustained NO releasing and not only because of chitosan properties [50,53].

5. Conclusions

In conclusion, this is a first attempt to identify the potential of NO-loaded chitosan nanoparticles in decreasing promastigote and amastigote forms de *L. (L.) amazonensis* without toxicity on macrophages. Low cost, biocompatibility and biodegradability make CS NPs very interesting to encapsulate NO donors. As this formulation is designed to treat CL, in practice, NONPs might be administrated directly to the infected wound by subcutaneous inoculation, or by incorporating the NP suspension into a cutaneous hydrogel, as previously proposed [54]. Additionally, there is clearly the possibility of developing new protocols involving different NONP concentrations and suitable number of applications. We envisage this innovative nanoplatform as a non-invasive and promising therapy for cutaneous leishmaniasis and hope to encourage further studies in this area.

Author contributions

All authors contributed equally in this manuscript.

Acknowledgements

We thank Prof. Silvia Reni Bortolin Uliana from University of São Paulo for providing the *L. (L.) amazonensis* transgenic line expressing luciferase strain. We also thank Conselho Nacional de Desenvolvimento Científico e Tecnológico (CNPq), Fundação de Amparo à Pesquisa do Estado de São Paulo (FAPESP) and Comissão Nacional de Energia Nuclear (CNEN) by financial support.

References

[1] M. Akhoundi, K. Kuhls, A. Cannet, et al., A historical overview of the classification, evolution, and dispersion of Leishmania parasites and sandflies, PLoS Neglected Trop. Dis. 10 (2016) e0004349.
[2] World Health Organization (WHO), Global Health Observatory (GHO) Data, (2019) http://www.who.int/gho/neglected_diseases/leishmaniasis/ , Accessed date: 20 March 2019.
[3] World Health Organization (WHO), Leishmaniasis. Epidemiological situatuion, http://www.who.int/leishmaniasis/burden/en, (2019) , Accessed date: 20 March 2019.
[4] M. Yanik, M.S. Gurel, Z. Simsek, et al., The psychological impact of cutaneous leishmaniasis, Clin. Exp. Dermatol. 29 (2004) 464–467.
[5] F. Bahrami, A.M. Harandi, S. Rafati, Biomarkers of cutaneous leishmaniasis, Front Cell Infect Microbiol 8 (2018) 222.
[6] A. Ponte-Sucre, F. Gamarro, J.C. Dujardin, et al., Drug resistance and treatment failure in leishmaniasis: a 21st century challenge, PLoS Neglected Trop. Dis. 11 (2017) e0006052.
[7] H.J.C. de Vries, S.H. Reedijk, H. Schallig, Cutaneous leishmaniasis: recent developments in diagnosis and management, Am. J. Clin. Dermatol. 16 (2015) 99–109.
[8] M.F. Horta, B.P. Mendes, E.H. Roma, et al., Reactive oxygen species and nitric oxide in cutaneous leishmaniasis, J. Parasitol. Res. 2012 (2012) 203818.
[9] X.Q. Wei, I.G. Charles, A. Smith, et al., Altered immune responses in mice lacking inducible nitric oxide synthase, Nature 375 (1995) 408–411.
[10] S. Stenger, N. Donhauser, H. Thuring, et al., Reactivation of latent leishmaniasis by inhibition of inducible nitric oxide synthase, J. Exp. Med. 183 (1996) 1501–1514.
[11] A. Diefenbach, H. Schindler, N. Donhauser, et al., Type 1 interferon (IFNalpha/beta) and type 2 nitric oxide synthase regulate the innate immune response to a protozoan parasite, Immunity 8 (1998) 77–87.
[12] P. Holzmuller, D. Sereno, M. Cavaleyra, et al., Nitric oxide-mediated proteasome-dependent oligonucleosomal DNA fragmentation in Leishmania amazonensis amastigotes, Infect. Immun. 70 (2002) 3727–3735.
[13] D.J. Suchyta, M.H. Schoenfisch, Encapsulation of N-diazeniumdiolates within liposomes for enhanced nitric oxide donor stability and delivery, Mol. Pharm. 12 (2015) 3569–3574.
[14] F. Butsch, B. Lorenz, A. Goldinger, et al., Topical treatment with a two-component gel releasing nitric oxide cures C57BL/6 mice from cutaneous leishmaniasis caused by Leishmania major, Exp. Dermatol. 25 (2016) 914–916.
[15] I.S. Costa, G.F. de Souza, M.G. de Oliveira, et al., S-nitrosoglutathione (GSNO) is cytotoxic to intracellular amastigotes and promotes healing of topically treated Leishmania major or Leishmania braziliensis skin lesions, J. Antimicrob. Chemother. 68 (2013) 2561–2568.
[16] G.F. de Souza, J.K. Yokoyama-Yasunaka, A.B. Seabra, et al., Leishmanicidal activity of primary S-nitrosothiols against Leishmania major and Leishmania amazonensis: implications for the treatment of cutaneous leishmaniasis, Nitric Oxide 15 (2006) 209–216.
[17] H.C. Oliveira, B.C. Gomes, M.T. Pelegrino, et al., Nitric oxide-releasing chitosan nanoparticles alleviate the effects of salt stress in maize plants, Nitric Oxide 61 (2016) 10–19.
[18] E. Moreno, J. Schwartz, C. Fernandez, et al., Nanoparticles as multifunctional devices for the topical treatment of cutaneous leishmaniasis, Expert Opin. Drug Deliv. 11 (2014) 579–597.
[19] D.S. Lima, B. Gullon, A.C. Cobas, Chitosan-based silver nanoparticles: a study of the antibacterial, antileishmanial and cytotoxic effects - Dimensions, J. Bioact. Compat Polym. 32 (2017) 397–410.
[20] M. Kong, X.G. Chen, K. Xing, H.J. Park, Antimicrobial properties of chitosan and mode of action: a state of the art review, Int. J. Food Microbiol. 144 (2010) 51–63.
[21] D. Zhao, S. Yu, B. Sun, S. Gao, S. Guo, K. Zhao, Biomedical applications of chitosan and its derivative nanoparticles, Polymers 10 (2018) E462.
[22] S. Naskar, K. Koutsu, S. Sharma, Chitosan-based nanoparticles as drug delivery systems: a review on two decades of research, J. Drug Target. 27 (2019) 379–393.
[23] M.T. Pelegrino, L.C. Silva, C.M. Watashi, et al., Nitric oxide-releasing nanoparticles: synthesis, characterization, and cytotoxicity to tumorigenic cells, J. Nanoparticle Res. 19 (2017) 57.
[24] M.T. Pelegrino, R.B. Weller, X. Chen, et al., Chitosan nanoparticles for nitric oxide delivery in human skin, Med. Chem. Commun. 8 (2017) 713–719.
[25] L.B. de Oliveira de Siqueira, V. da Silva Cardoso, I.A. Rodrigues, et al., Development and evaluation of zinc phthalocyanine nanoemulsions for use in photodynamic therapy for Leishmania spp, Nanotechnology 28 (2017) 065101.
[26] V.F. Cardozo, C.A. Lancheros, A.M. Narciso, et al., Evaluation of antibacterial activity of nitric oxide-releasing polymeric particles against Staphylococcus aureus and Escherichia coli from bovine mastitis, Int. J. Pharm. 473 (2014) 20–29.
[27] J.Q. Reimao, C.T. Trinconi, J.K. Yokoyama-Yasunaka, et al., Parasite burden in Leishmania (Leishmania) amazonensis-infected mice: validation of luciferase as a quantitative tool, J. Microbiol. Methods 93 (2013) 95–101.
[28] M. Cortez, C. Huynh, M.C. Fernandes, et al., Leishmania promotes its own virulence by inducing expression of the host immune inhibitory ligand CD200, Cell Host Microbe 9 (2011) 463–471.
[29] D.S. Zamboni, M. Rabinovitch, Nitric oxide partially controls coxiella burnetii phase II infection in mouse primary macrophages, Infect. Immun. 71 (2003) 1225–1233.
[30] R.C. Zauli-Nascimento, D.C. Miguel, J.K. Yokoyama-Yasunaka, et al., In vitro sensitivity of Leishmania (Viannia) braziliensis and Leishmania (Leishmania) amazonensis Brazilian isolates to meglumine antimoniate and amphotericin B, Trop. Med. Int. Health 15 (2010) 68–76.
[31] K. De Vos, Cell counter, https://imagej.nih.gov/ij/plugins/cell-counter.html.
[32] L.C. Green, D.A. Wagner, J. Glogowski, et al., Analysis of nitrate, nitrite, and nitrate in biological fluids, Anal. Biochem. 126 (1982) 131–138.
[33] S. Pandya, R.K. Verma, P. Khare, et al., Supplementation of host response by targeting nitric oxide to the macrophage cytosol is efficacious in the hamster model of visceral leishmaniasis and adds to efficacy of amphotericin B, Int. J. Parasitol. Drugs Drug Resist. 6 (2016) 125–132.
[34] L.M. Monteiro, R. Lobenberg, E.I. Ferreira, et al., Targeting Leishmania amazonensis amastigotes through macrophage internalisation of a hydroxymethylnitrofurazone nanostructured polymeric system, Int. J. Antimicrob. Agents 50 (2017) 88–92.
[35] M. Genestra, D. Guedes-Silva, W.J. Souza, et al., Nitric oxide synthase (NOS) characterization in Leishmania amazonensis axenic amastigotes, Arch. Med. Res. 37 (2006) 328–333.
[36] A.B. Seabra, G.Z. Justo, P.S. Haddad, State of the art, challenges and perspectives in the design of nitric oxide-releasing polymeric nanomaterials for biomedical applications, Biotechnol. Adv. 33 (2015) 1370–1379.
[37] J. Dolansky, et al., Antibacterial nitric oxide- and singlet oxygen-releasing polystyrene nanoparticles responsive to light and temperature triggers, Nanoscale 10 (2018) 2639–2648.
[38] A. Jones, J. Pant, E. Lee, M.J. Goudie, A. Gruzd, J. Mansfield, A. Mandal, S. Sharma, H. Handa, Nitric oxide-releasing antibacterial albumin plastic for biomedical applications, J. Biomed. Mater. Res. A 106 (2018) 1535–1542.
[39] M. Choi, S. Park, K. Park, H. Jeong, H. Jinkee, Nitric oxide delivery using biocompatible perfluorocarbon microemulsion for antibacterial effect, ACS Biomater. Sci. Eng. 5 (2019) 1378–1383.
[40] T. Hoang, Y. Lee, P. Le Thi, K.D. Park, Nitric oxide-releasing injectable hydrogels with high antibacterial activity through in situ formation of peroxynitrite, Acta Biomater. 67 (2018) 66–78.

[41] Z. Shariatinia, Pharmaceutical applications of chitosan, Adv. Colloid Interface Sci. 263 (2019) 131–194.
[42] K. Zhang, S.M. Beverley, Phospholipid and sphingolipid metabolism in Leishmania, Mol. Biochem. Parasitol. 170 (2010) 55–64.
[43] C.A. Henard, E.D. Carlsen, C. Hay, et al., Leishmania amazonensis amastigotes highly express a tryparedoxin peroxidase isoform that increases parasite resistance to macrophage antimicrobial defenses and fosters parasite virulence, PLoS Neglected Trop. Dis. 8 (2014) e3000.
[44] A.B. Seabra, N.A. Kitice, M.T. Pelegrino, et al., Nitric oxide-releasing polymeric nanoparticles against Trypanosoma cruzi, J. Phys. Conf. Ser. 617 (2015) 012020.
[45] J. Mauel, A. Ransijn, Leishmania spp.: mechanisms of toxicity of nitrogen oxidation products, Exp. Parasitol. 87 (1997) 98–111.
[46] JPd Menezes, E.M. Saraiva, Bd Rocha-Azevedo, The site of the bite: Leishmania interaction with macrophages, neutrophils and the extracellular matrix in the dermis, Parasites Vectors 9 (2016) 264.
[47] D.O. Schairer, J.S. Chouake, J.D. Nosanchuk, et al., The potential of nitric oxide releasing therapies as antimicrobial agents, Virulence (2012) 271–279.
[48] B.C. Smith, M.A. Marletta, Mechanisms of S-nitrosothiol formation and selectivity in nitric oxide signaling, Curr. Opin. Chem. Biol. 16 (2012) 498–506.
[49] J.L. Lemesre, D. Sereno, S. Daulouede, et al., Leishmania spp.: nitric oxide-mediated metabolic inhibition of promastigote and axenically grown amastigote forms, Exp. Parasitol. 86 (1997) 58–68.
[50] J. Wilson, C. Huynh, K.A. Kennedy, et al., Control of parasitophorous vacuole expansion by LYST/Beige restricts the intracellular growth of Leishmania amazonensis, PLoS Pathog. 4 (2008) e1000179.
[51] L. Soong, Subversion and utilization of host innate defense by Leishmania amazonensis, Front. Immunol. 3 (2012) 58.
[52] P.E. Kima, The amastigote forms of Leishmania are experts at exploiting host cell processes to establish infection and persist, Int. J. Parasitol. 37 (2007) 1087–1096.
[53] F. Real, R.A. Mortara, M. Rabinovitch, Fusion between Leishmania amazonensis and Leishmania major parasitophorous vacuoles: live imaging of coinfected macrophages, PLoS Neglected Trop. Dis. 4 (2010) e905.
[54] M.T. Pelegrino, D.R. de Araújo, A.B. Seabra, S-nitrosoglutathione-containing chitosan nanoparticles dispersed in Pluronic F-127 hydrogel: potential uses in topical applications, J. Drug Deliv. Sci. Technol. 43 (2018) 211–220.